Separation Science and Technology
Publication details, including instructions for authors and subscription information:
http://www.informaworld.com/smpp/title~content=t713708471

Influence of Temperature Gradients on Velocity Profiles and Separation Parameters in Thermal Field-Flow Fractionation

Judy J. Gunderson[a]; Karin D. Caldwell[a]; J. Calvin Giddings[a]
[a] DEPARTMENT OF CHEMISTRY, UNIVERSITY OF UTAH, SALT LAKE CITY, UTAH

To cite this Article Gunderson, Judy J. , Caldwell, Karin D. and Giddings, J. Calvin(1984) 'Influence of Temperature Gradients on Velocity Profiles and Separation Parameters in Thermal Field-Flow Fractionation', Separation Science and Technology, 19: 10, 667 — 683
To link to this Article: DOI: 10.1080/01496398408060668
URL: http://dx.doi.org/10.1080/01496398408060668

SEPARATION SCIENCE AND TECHNOLOGY, 19(10), pp. 667-683, 1984

Influence of Temperature Gradients on Velocity Profiles and Separation Parameters in Thermal Field-Flow Fractionation

JUDY J. GUNDERSON, KARIN D. CALDWELL, and J. CALVIN GIDDINGS

DEPARTMENT OF CHEMISTRY
UNIVERSITY OF UTAH
SALT LAKE CITY, UTAH 84112

Abstract

The form of the asymmetrical velocity profile present in thermal field-flow fractionation is investigated. A theoretical treatment of retention and nonequilibrium peak broadening is given for an exponential concentration profile combined with the asymmetrical velocity profile. The different consequences of the symmetrical and asymmetrical velocity profiles are discussed.

INTRODUCTION

Field-flow fractionation (FFF) is a separation technique which is based on the exposure of a sample to the combined effects of an external field applied perpendicular to the axis of a fractionation channel and the axial flow of carrier liquid through the open channel. The field interacts with the various components of the sample, causing their migration toward the channel wall. The carrier flows laminarly with the fastest flowlines located in or near the middle of the parallel plate-type channel, and sluggish flow in the vicinity of the walls. Species which are forced to concentrate near the wall due to a strong interaction with the field will move downstream with relatively slow velocities, thus being retained longer than those species with weaker field interactions.

FFF retention therefore depends not only on the applied field but also on the distribution of flow velocities in the channel, i.e., the flow velocity profile.

0149-6395/84/1910-0667$3.50/0

For fields such as electrical (*1*) or sedimentation (*2*), one may safely assume the velocity profile to be parabolic with the maximum flow velocity found exactly at the midpoint of the channel. This assumption is not correct in the case of thermal FFF, which relies on rather steep temperature gradients to achieve separation. Since the viscosity of most carrier liquids is a strong function of the temperature, and thus of position in the channel, the velocity profile will no longer be symmetrical around the center of the channel.

In the initial development of thermal FFF theory (*3*), the flow profile was treated as parabolic; later refinements introduced a simple temperature correction to the viscosity which, although treated inaccurately, permitted exploration of the effects that a skewed velocity profile has on retention (*4*). An exact solution to the equation of motion for laminar flow between infinite parallel plates of different temperatures was presented by Westerman-Clark (*5*). In solving the equation he assumes a linear temperature gradient between the plates and an exponential dependence of the viscosity on temperature. The practical application of his derivation is hindered due to the presence of an exponential integral in his solution. In the present work we will derive an exact and implicit solution employing slightly more general assumptions based on appropriate series expansion which are stated in the text. The resulting solution will lend itself to convenient evaluation under a variety of experimental conditions. We will then find general equations describing retention parameters and apply them to specific solvents and temperature differentials which are frequently used in thermal FFF.

The refinement of theories for retention and plate height will ultimately obviate the need for calibration curves which are employed whenever the thermal FFF technique is used for polymer characterization. It will instead permit direct first principles interpretation of observed fractograms in terms of relevant physical parameters, i.e., diffusivity, thermal diffusivity, and molecular weight of the sample.

THEORY

Under the assumption of uniform flow in the longitudinal dimension of an infinite parallel plate channel, the equation of motion is of the form (*5*)

$$\eta(x)\frac{d^2v(x)}{dx^2} + \frac{d\eta(x)}{dx}\frac{dv(x)}{dx} = \frac{-\Delta p}{L} \tag{1}$$

where $v(x)$ is the velocity at position x in the channel, $\eta(x)$ is the position-dependent liquid viscosity, and $\Delta p/L$, a positive quantity, is the pressure

increment per unit length of the channel. The velocity profile is found, through integration, to be

$$v(x) = \frac{-\Delta p}{L}\left[\int_0^x \frac{x}{\eta(x)}\,dx + \theta\int_0^x \frac{1}{\eta(x)}\,dx + a\right] \tag{2}$$

where a and θ are constants of integration which may be evaluated from the boundary conditions specifying zero velocity at the two channel walls, i.e., at $x = 0$ and $x = w$. This results in the following equation for the generalized velocity profile:

$$v(x) = \frac{-\Delta p}{L}\left[\int_0^x \frac{x}{\eta(x)}\,dx - \frac{\left(\int_0^w \frac{x}{\eta(x)}\,dx\right)}{\left(\int_0^w \frac{1}{\eta(x)}\,dx\right)}\left(\int_0^x \frac{1}{\eta(x)}\,dx\right)\right] \tag{3}$$

The basis for fractionation in thermal FFF is the existence of a temperature gradient across the channel. Since liquid viscosities $\eta(T)$ are strongly temperature dependent, the temperature profile gives a position dependence to the viscosity expressed as $\eta(x)$. In order to determine $\eta(x)$ and thus solve Eq. (3), we must do two things: we must first determine the temperature dependence of the viscosity, or more appropriately its inverse, the fluidity, and we must second determine the form of the temperature profile so that the temperature dependence $\eta(T)$ can be converted into the distance dependence $\eta(x)$.

The temperature dependence of fluidity is readily accounted for by fitting fluidity data (*6–11*) to a polynomial function. Experimental data for ethylbenzene, tetrahydrofuran, and 1,2-dichloroethane were found to fit a cubic equation very well over the temperature ranges of interest (Fig. 1):

$$\frac{1}{\eta} = a_0 + a_1 T + a_2 T^2 + a_3 T^3 \tag{4}$$

The temperature dependence of the fluidity has often been expressed as an exponential (*11*), but the exponential fit is not as good as the above cubic expression over the temperature range of interest here, and is not as convenient for integration.

In the past a linear temperature gradient across the channel has often been assumed (*4*). This is only correct to a first approximation since the

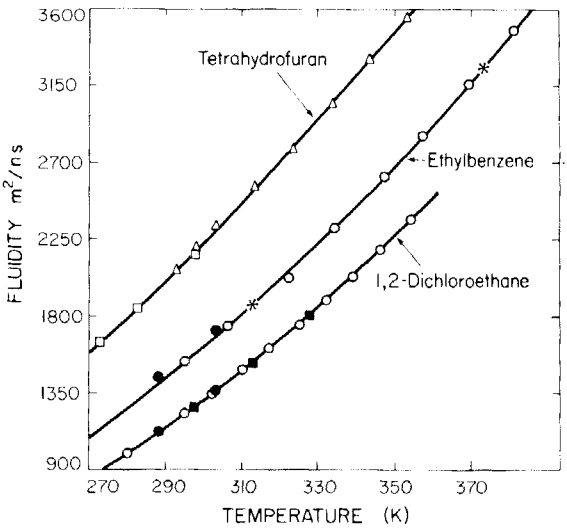

FIG. 1. Comparison of fluidity predicted by Eq. (4) and experimental values: (△) Ref. 6, (□) Ref. 7, (○) Ref. 8, (●) Ref. 9, (■) Ref. 10, (*) Ref. 11. Equations for the solvents are:

$$\text{Ethylbenzene: } \frac{1}{\eta} = -6059.42 + 47.5888T - 0.12525T^2 + 1.73452 \times 10^{-4} T^3$$

$$\text{Tetrahydrofuran: } \frac{1}{\eta} = 7622.73 - 88.9325T + 0.33440T^2 - 3.25866 \times 10^{-4} T^3$$

$$\text{1,2-Dichloroethane: } \frac{1}{\eta} = 679.57 - 11.8324T + 4.39798 \times 10^{-2} T^2 + 8.26069 \times 10^{-4} T^3$$

temperature gradient at any point is a function of the thermal conductivity of the liquid, and the thermal conductivity, in turn, varies with the temperature. This will result in a nonlinear temperature profile. The thermal conductivity of nonpolar liquids may be approximated by the expression (*11, 12*)

$$\kappa = \kappa_c + \frac{d\kappa}{dT}(T - T_c) \tag{5}$$

where κ is the thermal conductivity at temperature T and κ_c is the value of κ at the cold wall temperature T_c. We will assume $d\kappa/dT$ to be constant over our working temperature ranges (*11, 12*). The temperature gradient may then be written as (*12*)

$$\frac{dT}{dx} = \frac{q}{\kappa} = \frac{q}{\kappa_c \left[1 + \frac{1}{\kappa_c} \frac{d\kappa}{dT} (T - T_c)\right]} \tag{6}$$

where the constant q (formerly A in Ref. *12*) is the heat flow through a unit area of the system; for a given set of conditions, q is determined as (*12, 13*)

$$\frac{q}{\kappa_c} = \frac{1}{w} \left(\Delta T + \frac{1}{\kappa_c} \frac{d\kappa}{dT} \frac{(\Delta T)^2}{2}\right) = \frac{S}{w} \tag{7}$$

where ΔT is the temperature drop across the channel and S is a constant. Through manipulation of Eqs. (6) and (7), the temperature at any position in the channel can be determined by the equation (*13*)

$$T(x) = T_c + \frac{-1 + \left[1 + \frac{2x}{w} \frac{1}{\kappa_c} \frac{d\kappa}{dT} \Delta T + \frac{x}{w} \left(\frac{1}{\kappa_c} \frac{d\kappa}{dT}\right)^2 (\Delta T)^2\right]^{1/2}}{\frac{1}{\kappa_c} \frac{d\kappa}{dT}} \tag{8}$$

Although the equation is an exact solution for the temperature profile based on Eq. (5), it is a complicated function of x. If we substituted this equation into Eq. (4) so as to have the fluidity as a function of x, the velocity expression would become quite cumbersome. Instead, we will seek a simpler approximation for the temperature profile. We start by expanding the temperature in a Taylor's series about the cold wall ($x = 0$):

$$T(x) = T_c + x \left(\frac{dT}{dx}\right)_c + \frac{x^2}{2} \left(\frac{d^2T}{dx^2}\right)_c + \frac{x^3}{3!} \left(\frac{d^3T}{dx^3}\right)_c + \cdots \tag{9}$$

The temperature gradient dT/dx has been described in Eq. (6) and is evaluated at the cold wall as

$$\left(\frac{dT}{dx}\right)_c = \frac{q}{\kappa_c} = \frac{S}{w} \tag{9a}$$

From Eq. (6) we also determine the higher-order derivatives at the cold wall:

$$\left(\frac{d^2T}{dx^2}\right)_c = -\left(\frac{S}{w}\right)^2\left(\frac{1}{\kappa_c}\right)\left(\frac{d\kappa}{dT}\right)_c \tag{9b}$$

$$\left(\frac{d^3T}{dx^3}\right)_c = -\left(\frac{S}{w}\right)^3\left(\frac{1}{\kappa_c}\right)\left[\left(\frac{d^2\kappa}{dT^2}\right)_c - \frac{2}{\kappa_c}\left(\frac{d\kappa}{dT}\right)_c^2\right] \tag{9c}$$

Assuming $d\kappa/dT$ to be a constant and substituting Eqs. (9a), (9b), and (9c) into Eq. (9), we get the following equation for the temperature profile:

$$T(x) = T_c + S\left(\frac{x}{w}\right) - \frac{1}{2}\frac{S^2}{\kappa_c}\left(\frac{d\kappa}{dT}\right)\left(\frac{x}{w}\right)^2 + \frac{1}{3}\frac{S^3}{\kappa_c^2}\left(\frac{d\kappa}{dT}\right)^2\left(\frac{x}{w}\right)^3 \tag{10}$$

where the equation is written in terms of the reduced parameter x/w. Comparison of Eq. (10) to Eq. (8) (see Table 1 and Fig. 2) shows that the cubic expansion is a good approximation to the exact solution for the conditions and heat fluxes of interest in this work.

By introducing Eq. (10) into Eq. (4), we have a polynomial relationship for fluidity in terms of channel position. This polynomial is truncated after

TABLE 1
Evaluation of Approximate Relationships between Temperature T and Reduced Position Coordinate x/w for Ethylbenzene at $T_c = 20°C$ and $\Delta T = 100°C$:

$$T_1 = T_c + S\frac{x}{w}$$

$$T_2 = T_1 - \frac{1}{2}\frac{S^2}{\kappa_c}\left(\frac{d\kappa}{dT}\right)\left(\frac{x}{w}\right)^2$$

$$T_3 = T_2 + \frac{1}{3}\frac{S^3}{\kappa_c^2}\left(\frac{d\kappa}{dT}\right)^2\left(\frac{x}{w}\right)^3$$

T_{comp} Represents the Values Predicted by Eq. (8)

x/w	T_1 (°C)	T_2 (°C)	T_3 (°C)	T_{comp} (°C)
0.0	20.0	20.0	20.0	20.0
0.1	29.1	29.2	29.2	29.2
0.2	38.2	38.5	38.5	38.5
0.3	47.2	47.9	47.9	47.9
0.5	65.4	67.3	67.4	67.5

four terms. The maximum error in this equation, 3% for ethylbenzene at $\Delta T = 100°C$, occurs at the hot wall and will perturb the velocity profile only slightly. In FFF the field tends to concentrate the sample molecules in the cold wall region and in this region, i.e., $0 \leq x/w \leq 0.5$, the four term polynomial expression introduces errors of less than 0.25% in the fluidity. The fluidity as a function of channel position is

$$\frac{1}{\eta} = b_0 + b_1 \frac{x}{w} + b_2 \left(\frac{x}{w}\right)^2 + b_3 \left(\frac{x}{w}\right)^3 \tag{11}$$

where

$$b_0 = a_3 T_c^3 + a_2 T_c^2 + a_1 T_c + a_0 \tag{11a}$$

$$b_1 = (3T_c^2 a_3 + 2T_c a_2 + a_1)S \tag{11b}$$

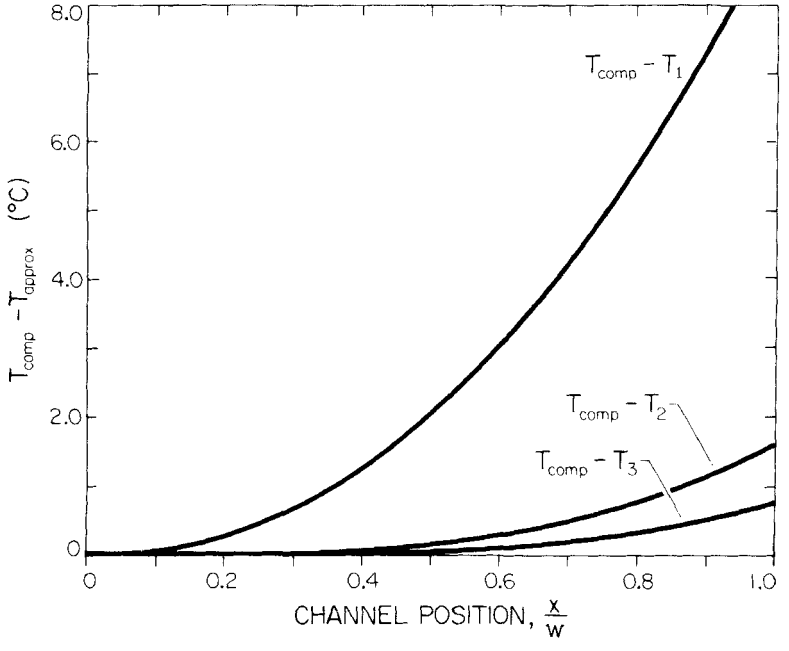

FIG. 2. Differences between the exact solution based on Eq. (5), T_{comp}, and various approximate temperatures, T_1, T_2, T_3, given in Table 1, as a function of reduced channel position. The temperatures are calculated for ethylbenzene at $T_c = 20°C$ and $\Delta T = 100°C$.

$$b_2 = \left(3T_c a_3 - \frac{3}{2} T_c^2 \frac{1}{\kappa_c} \frac{d\kappa}{dT} a_3 - T_c \frac{1}{\kappa_c} \frac{d\kappa}{dT} a_2 + a_2 - \frac{1}{2} \frac{1}{\kappa_c} \frac{d\kappa}{dT} a_1\right) S^2 \tag{11c}$$

$$b_3 = \left[T_c^2 \left(\frac{1}{\kappa_c} \frac{d\kappa}{dT}\right)^2 a_3 - 3T_c \frac{1}{\kappa_c} \frac{d\kappa}{dT} a_3 + a_3 + \frac{2}{3} T_c \left(\frac{1}{\kappa_c} \frac{d\kappa}{dT}\right)^2 a_2 - \frac{1}{\kappa_c} \frac{d\kappa}{dT} a_2 + \frac{1}{3} \left(\frac{1}{\kappa_c} \frac{d\kappa}{dT}\right)^2 a_1 \right] S^3 \tag{11d}$$

Combining Eqs. (11) and (3), and performing the necessary integrations, we get the velocity profile

$$v(x) = \frac{-\Delta p}{L} \left[\theta b_0 \frac{x}{w} + \frac{1}{2}(b_0 + \theta b_1)\left(\frac{x}{w}\right)^2 + \frac{1}{3}(b_1 + \theta b_2)\left(\frac{x}{w}\right)^3 + \frac{1}{4}(b_2 + \theta b_3)\left(\frac{x}{w}\right)^4 + \frac{1}{5} b_3 \left(\frac{x}{w}\right)^5 \right] \tag{12}$$

where

$$\theta = -\left(\frac{b_0}{2} + \frac{b_1}{3} + \frac{b_2}{4} + \frac{b_3}{5}\right) \Big/ \left(b_0 + \frac{b_1}{2} + \frac{b_2}{3} + \frac{b_3}{4}\right) \tag{12a}$$

We will rewrite the equation for simplicity as

$$v(x) = \frac{-\Delta p}{L} \left[h_1 \left(\frac{x}{w}\right) + h_2 \left(\frac{x}{w}\right)^2 + h_3 \left(\frac{x}{w}\right)^3 + h_4 \left(\frac{x}{w}\right)^4 + h_5 \left(\frac{x}{w}\right)^5 \right] \tag{13}$$

In order to compare velocity profiles generated under different experimental conditions, we need to normalize the velocity profile by dividing $v(x)$ by its average value $\langle v(x) \rangle$ which is found to be

$$\langle v(x) \rangle = \frac{-\Delta p}{L} \left[\frac{h_1}{2} + \frac{h_2}{3} + \frac{h_3}{4} + \frac{h_4}{5} + \frac{h_5}{6}\right] = \frac{-\Delta p}{L} \sum_{i=1}^{5} \frac{h_i}{(i+1)} \tag{14}$$

The distortion of the velocity profile, which arises from the thermal gradient and its resulting distribution of viscosities, is demonstrated in Fig. 3. The isoviscous case is compared to Eq. (12) for ethylbenzene with $T_c = 20°C$ and $\Delta T = 100°C$. The decreased velocity near the cold wall is due to the fact that the viscosity is highest at that point.

In the limit of no temperature dependence in the viscosity ($b_i = 0$ for $i \geq 1$), the normalized velocity profile takes the symmetrical parabolic form used in the development of the general theory of FFF (*3*):

$$\frac{v(x)}{\langle v(x)\rangle} = 6\left[\frac{x}{w} - \left(\frac{x}{w}\right)^2\right] \tag{15}$$

RETENTION EQUATION

As in chromatography, the retention parameter R in FFF is defined as the ratio of the solute zonal velocity to the average velocity of the solvent. This ratio may be expressed as

$$R = \frac{\langle c(x)v(x)\rangle}{\langle c(x)\rangle\langle v(x)\rangle} \tag{16}$$

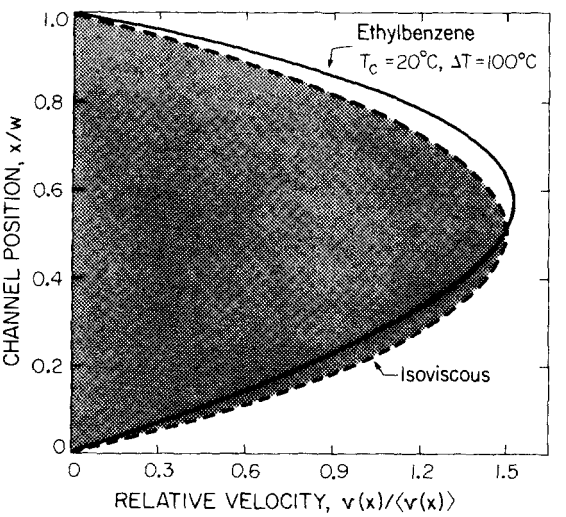

FIG. 3. Asymmetry of the velocity profile for ethylbenzene at $T_c = 20°C$ and $\Delta T = 100°C$ according to Eq. (13). The isoviscous symmetrical velocity profile (Eq. 15) is shown for comparison.

where c is the solute concentration and the angled parentheses denote cross-sectional averages. The concentration profile is determined by examining the flux equation for a solute in a thermal gradient (*4, 14*):

$$J_x = -D\left[\frac{dc}{dx} + c\left(\frac{\alpha}{T} + \gamma\right)\frac{dT}{dx}\right] \tag{17}$$

where D is the diffusion coefficient, γ is the cubic coefficient of thermal expansion, and α is the thermal diffusion factor. Letting J_x equal zero under the steady-state assumption results in the equation

$$\frac{1}{c}\frac{dc}{dx} = -\left(\frac{\alpha}{T} + \gamma\right)\frac{dT}{dx} \tag{18}$$

In order to find the concentration distribution $c(x)$ as a function of position coordinate x, it is convenient to make some simplifying assumptions about the terms on the right-hand side of the equation. First, we will consider the two terms within the parentheses, α/T and γ. Since γ is a small term compared to α/T, we will neglect it. The right-hand side of the equation then becomes the product $(\alpha/T) \times (dT/dx)$; it is the temperature dependence of this product with which we will be concerned. Each of the two terms in the product is temperature dependent; α/T decreases with increasing temperature (*12, 13*) whereas dT/dx increases with increasing temperature due to its inverse dependence on thermal conductivity (Eq. 6). Although the terms in the product will compensate each other to some extent, α/T has the stronger temperature dependence of the two. The temperature dependence of each of the terms and of the product is shown in Fig. 3. While the temperature dependence of the product is significant, the temperature range over which the solute zone extends is not large. Thus, only a small portion of the temperature range shown in Fig. 4 is experienced by solute molecules. For example, in a highly unfavorable case, a mildly retained sample ($R = 0.5$) in ethylbenzene with a cold wall temperature T_c of 20°C and a hot wall temperature of 120°C is distributed such that 85% of the sample is spread over a 24.6°C range. This difference would result in a product term that varied by 17% over the 24.6°C range. At the other end of the spectrum a highly retained sample ($R = 0.1$) under the same conditions, except with a hot wall temperature of 45°C, is distributed such that 85% of the sample is spread over less than a 1°C range. This difference would result in a product term that varied by 0.75%. Thus we may assume the product on the right-hand side of Eq. (18) to be temperature independent without incurring a large error for moderately or highly retained species.

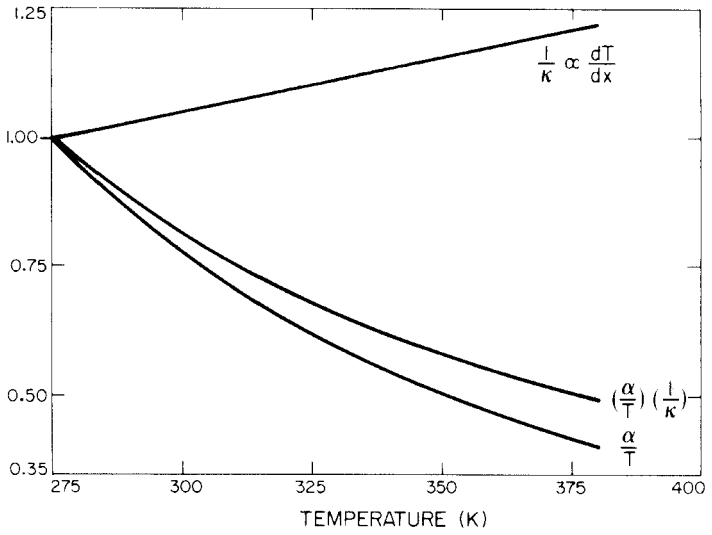

FIG. 4. Temperature dependence of (α/T), (dT/dx), and $(\alpha/T)(dT/dx)$ normalized to the values at 275 K for ethylbenzene at $T_c = 20°C$ and $\Delta T = 100°C$.

Upon solving the differential equation, the resulting concentration profile is of the form

$$c(x) = c_0 \exp\left(\frac{-x}{l}\right) \tag{19}$$

where c_0 is the concentration at the cold wall and constant $1/l$, where l approximates the mean thickness of the zone, is defined by

$$\frac{1}{l} = \left(\frac{\alpha}{T} + \gamma\right)\frac{dT}{dx} \tag{20}$$

The cross-sectional average concentration in the zone becomes

$$\langle c(x)\rangle = c_0\lambda(1 - e^{-1/\lambda}) \tag{21}$$

where λ is the dimensionless retention parameter defined as l/w.

Inserting Eqs. (13), (14), (19), and (21) into the expression for R (Eq. 16) we get

$$R = \frac{1}{\sum_{i=1}^{5} \frac{h_i}{(i+1)}} \left\{ \frac{1}{(1-e^{1/\lambda})} \left[\sum_{i=1}^{5} h_i \sum_{j=0}^{i-1} \frac{i!}{(i-j)!} \lambda^j \right] + \sum_{i=1}^{5} i! h_i \lambda^i \right\} \tag{22}$$

which, in the limit $\lambda \to 0$, assumes the form

$$R = \frac{\lambda}{\sum_{i=1}^{5} \frac{h_i/h_1}{(i+1)}} \tag{22a}$$

The retention determined from Eq. (22) is greater than that corresponding to a parabolic velocity profile (isoviscous case), as illustrated by the specific case shown in Fig. 5. This reflects the reduced flow velocity near the cold wall.

One of the goals of thermal FFF is the determination of the thermal diffusion parameters from observations of retention collected for various macromolecules. As shown in Eq. (22), we have a relationship between the

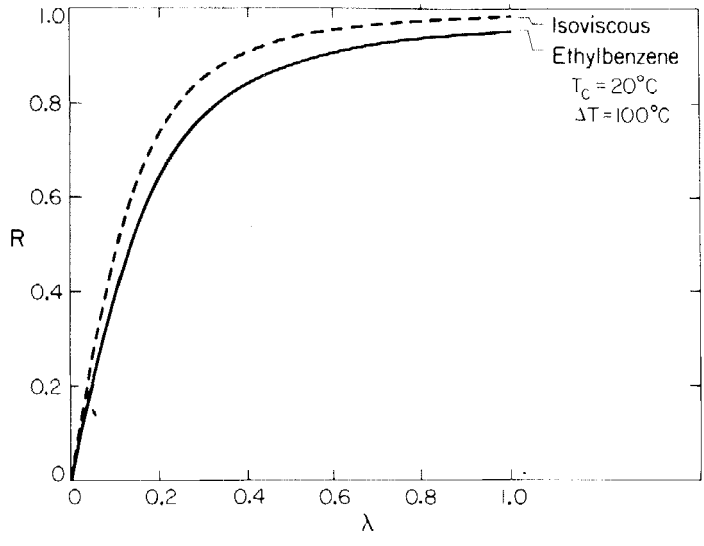

FIG. 5. Retention ratio R as a function of λ for the isoviscous system (Ref. 4, Eq. 5) and ethylbenzene at $T_c = 20°C$ and $\Delta T = 100°C$ according to Eq. (22).

observed retention R and λ; Eq. (20) in turn relates $l = \lambda w$ to α. Thus, if we measure the retention ratio for a specific material, we may determine its thermal diffusion factor α. This relationship between R and α is illustrated in Fig. 6 for ethylbenzene with $T_c = 20°C$ and $\Delta T = 100°C$.

ZONE BROADENING

A perturbation of the parabolic velocity profile affects not only the zonal retention but band broadening as well. The nonequilibrium contribution to the plate height expression in FFF has been treated in detail for the case of unperturbed parabolic flow (*15–17*) and has the form

$$H_n = \frac{\chi w^2 \langle v \rangle}{D} \tag{23}$$

where the parameter χ is a complicated function of λ or R (*15, 16*). An approximation for χ has been developed by Martin et al. (*17*); it is based on a third-degree polynomial expression for the velocity profile with one adjustable parameter ν:

$$\frac{v}{\langle v \rangle} = 6\left[(1+\nu)\left(\frac{x}{w}\right) - (1+3\nu)\left(\frac{x}{w}\right)^2 + 2\nu\left(\frac{x}{w}\right)^3\right] \tag{24}$$

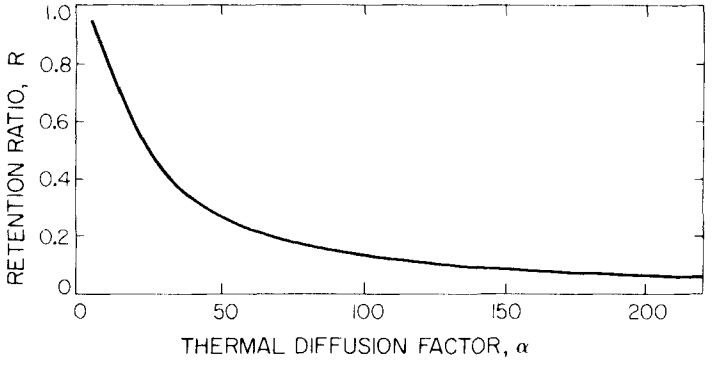

FIG. 6. Dependence of R on the thermal diffusion factor α for ethylbenzene at $T_c = 20°C$ and $\Delta T = 100°C$.

The resulting equation for χ is of the form (*17*)

$$\chi = \frac{2\lambda^2 F}{R(1 - e^{-1/\lambda})} \tag{25}$$

where

$$\begin{aligned} F = 2A[&6(1+\nu) - (1/\lambda) - (A/\lambda) + 36\nu\lambda^2 \\ &- 6\lambda(1+6\nu) + 18\lambda e^{-1/\lambda}(1+10\nu\lambda)] \\ &+ 72\lambda^2[(1+\nu)^2 - 10(1+4\nu+3\nu^2)\lambda \\ &+ 4(7+69\nu+90\nu^2)\lambda^2 - 672\nu(1+3\nu)\lambda^3 \\ &+ 4464\nu^2\lambda^4] - 72\lambda^2 e^{-1/\lambda}[7 - 2\nu + \nu^2 \\ &+ 2(5 - 68\nu + 15\nu^2)\lambda + 4(7 - 69\nu + 180\nu^2)\lambda^2 \\ &- 672\nu(1-3\nu)\lambda^3 + 4464\nu^2\lambda^4] \end{aligned} \tag{25a}$$

and

$$A = 12\lambda e^{-1/\lambda}(6\nu\lambda - 1)/(1 - e^{1/\lambda}) \tag{25b}$$

In order to examine the effect on band broadening due to a thermally distorted velocity profile, we generated a set of data from Eq. (13) describing the velocity profile of ethylbenzene with $T_c = 20°C$ and $\Delta T = 100°C$. We then fit this data to a third-degree polynomial by means of a least-squares analysis. As seen in Fig. 7, the fit is quite good. This is also indicated by an error of only 3.3% in the slope of the third-degree polynomial at the cold wall. This precision may be improved by performing a weighted fit of the data near the cold wall.

The expression for the nonequilibrium coefficient χ given by Eq. (25) may now be evaluated and compared to the isoviscous case. The comparison is shown in Fig. 8. For a mildly retained material the skewed velocity profile has a larger contribution to band broadening than the parabolic profile whereas for a highly retained material the skewed velocity profile has a smaller contribution to band broadening than the parabolic profile (not obvious in Fig. 8). This apparent contradiction arises due to the influence the slope of the velocity profile has on band broadening. The steeper the velocity profile is over the area of the solute zone, the greater the band broadening of the zone. At the cold wall the parabolic velocity profile is steeper than the skewed profile. Thus a highly retained sample experiences greater band

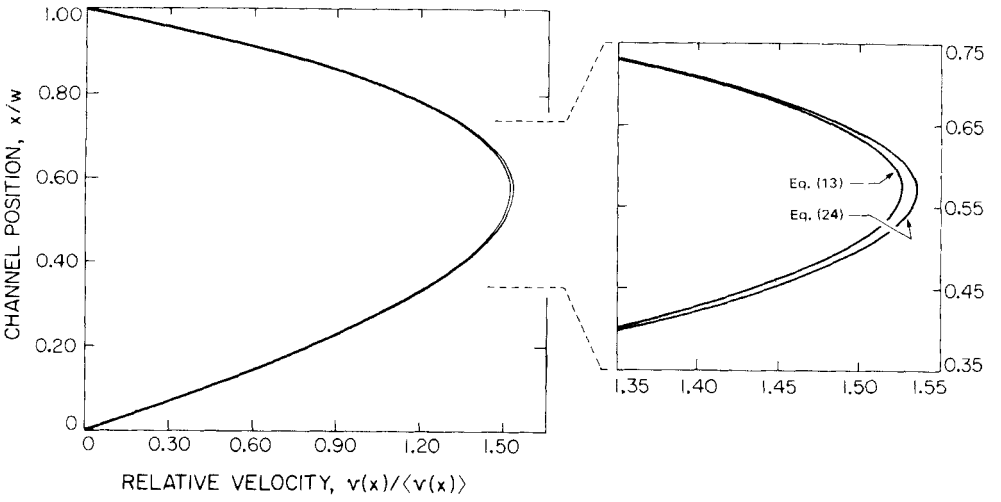

FIG. 7. The velocity profile according to Eq. (13) and the cubic approximation to it (Eq. 24) for ethylbenzene at $T_c = 20°C$ and $\Delta T = 100°C$.

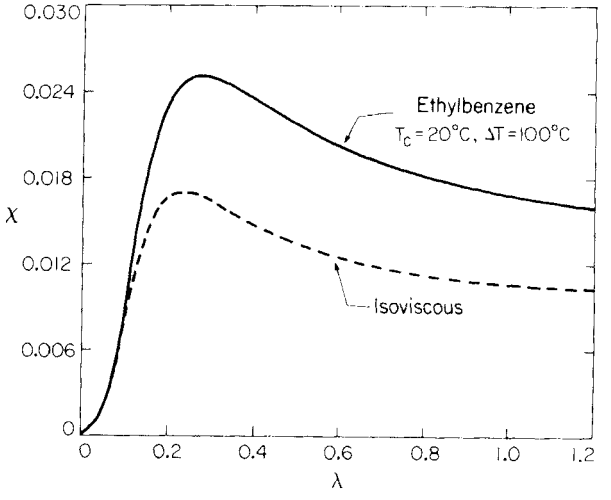

FIG. 8. Dependence of χ on λ for the isoviscous system (Ref. *16*, Eq. 26) and for ethylbenzene at $T_c = 20°C$ and $\Delta T = 100°C$ (Eq. 25).

broadening in a parabolic flow profile than in the skewed profile. For a lesser retained material the solute zone will begin extending into flow regions in the channel where the distorted flow profile has the steeper velocity gradient. Consequently, the distorted velocity profile will increase the band broadening of a mildly retained material.

SUMMARY AND CONCLUSIONS

The temperature profile across a thermal FFF channel has been shown to be accurately described by a polynomial in position coordinate x, where x represents the distance from the cold wall. This profile is based largely on empirical relationships between temperature and viscosity for various solvents. These relationships make it possible to express the inverse viscosities, i.e., the fluidities, of the solvents as functions of position coordinate x in the channel. The velocity profile across the channel was then found as the solution to the equation of motion of the fluid between infinite parallel plates. The resulting expression for the velocity profile is a polynomial in x, where the coefficients are evaluated in terms of known experimental parameters. This evaluation may be carried out by simple computer routines. (Information on computer routines is available from the authors.) The distortion in the velocity profile induced by the temperature gradient is demonstrated graphically for a set of typical experimental conditions.

The impact of the skewed velocity profile on retention was then examined. The solute was assumed to be exponentially distributed with respect to the cold wall during fractionation. Although the exponential expression is not exact, it is acceptable for moderately or highly retained species. Thus it was possible to estimate the effect of the skewed velocity profile on retention for different experimental conditions. The impact of this correction is illustrated by comparison with retention calculated for the parabolic velocity profile. The parabolic profile is characteristic of most forms of FFF.

The aim of sample characterization in FFF is to correctly describe the field-induced solute distribution in the channel, since this distribution is uniquely determined by the physical properties of the sample. In order to accurately relate an experimentally observed retention to the appropriate sample distribution, one must have access to an accurate velocity profile. It is this primary need which prompted the current study. We have also examined the implications of the skewed velocity profile on nonequilibrium zone broadening in the thermal FFF channel.

It will be the goal of future work to more accurately describe the sample distribution in a channel under the influence of a temperature gradient. This should provide an improved relationship between experimental retention and the thermal diffusion parameters for the sample.

Acknowledgments

This research was supported by National Science Foundation Grant No. CHE-8218503. Drs Michel Martin and Steve Brimhall are gratefully acknowledged for their work in the initial stages of this study.

REFERENCES

1. L. F. Kesner, K. D. Caldwell, M. N. Myers, and J. C. Giddings, *Anal. Chem., 48*, 1834 (1976).
2. G. Karaiskakis, M. N. Myers, K. D. Caldwell, and J. C. Giddings, *Ibid., 53*, 1314 (1981).
3. E. Grushka, K. D. Caldwell, M. N. Myers, and J. C. Giddings, *Sep. Purif. Methods, 2*, 129 (1973).
4. M. N. Myers, K. D. Caldwell, and J. C. Giddings, *Sep. Sci., 9*, 47 (1974).
5. G. Westerman-Clark, *Sep. Sci. Technol., 13*, 819 (1978).
6. E. Kuss, *Z. Angew. Phys., 7*, 372 (1955).
7. C. Carvayal, K. J. Tolle, J. Smid, and M. Szwarc, *J. Am. Chem. Soc., 87*, 5548 (1965).
8. T. E. Thorpe and J. W. Rodger, *Philos. Trans. R. Soc., 185*, 397 (1894).
9. J. Timmerman and F. Martin, *J. Chim. Phys., 23*, 733 (1926).
10. V. M. Heston, E. J. Hennely, and C. P. Smith, *J. Am. Chem. Soc., 70*, 4102 (1958).
11. R. C. Reid, J. M. Prausnitz, and T. K. Sherwood, *The Properties of Gases and Liquids*, 3rd ed., McGraw-Hill, New York, 1977.
12. J. C. Giddings, K. D. Caldwell, and M. N. Myers, *Macromolecules, 9*, 106 (1976).
13. S. L. Brimhall, PhD Dissertation, University of Utah, Salt Lake City, Utah, 1983.
14. M. E. Hovingh, G. H. Thompson, and J. C. Giddings, *Anal. Chem., 42*, 195 (1970).
15. J. C. Giddings, *J. Chem. Phys., 49*, 81 (1968).
16. J. C. Giddings, Y. H. Yoon, K. D. Caldwell, M. N. Myers, and M. E. Hovingh, *Sep. Sci., 10*, 447 (1975).
17. M. Martin and J. C. Giddings, *J. Phys. Chem., 85*, 72 (1981).